Two-photon upconversion affected by intermolecule correlations near metallic nanostructures

Yoshiki Osaka,[*] Nobuhiko Yokoshi,[†] and Hajime Ishihara

Department of Physics and Electronics, Osaka Prefecture University, 1-1 Gakuen-cho, Sakai, Osaka 599-8531, Japan
(Received 25 February 2016; published 18 April 2016)

We investigate an efficient two-photon upconversion process in more than one molecule coupled to an optical antenna. In the previous paper [Y. Osaka *et al.*, Phys. Rev. Lett. **112**, 133601 (2014)], we considered the two-photon upconversion process in a single molecule within one-dimensional input-output theory and revealed that controlling the antenna-molecule coupling enables the efficient upconversion with radiative loss in the antenna suppressed. In this paper, aiming to propose a way to enhance the total probability of antenna-photon scattering, we extend the model to the case of multiple molecules. In general, the presence of more than one molecule decreases the upconversion probability because they equally share the energy of the two photons. However, it is shown that we can overcome the difficulty by controlling the intermolecule coupling. Our result implies that, without increasing the incident photon number (light power), we can enlarge the net probability of the two-photon upconversion.

I. INTRODUCTION

Utilizing absorption saturation of discrete levels in nanomaterials such as molecules and quantum dots is a useful way to enhance optical nonlinearities by few photons [1]. However, it is necessary to supplement small absorption cross sections of nanomaterials for photons with auxiliary systems because the size of nanomaterials is tiny compared to the spatial extent of photon wave functions. Optical cavity is well known as an example of the auxiliary system to enhance interactions between photons and nanomaterials [2,3]. Another approach is to introduce an optical antenna that consists of metallic nanostructures. It produces electric fields localized beyond the diffraction limit near the metal surface by localized surface plasmon resonance [4,5]. By embedding the nanomaterials near the optical antenna, the nanomaterials strongly interact with the localized fields [6,7]. Especially when metallic nanostructures are set at intervals of a few nanometers, there exists a "hot spot" near the gap region where the field intensity is enhanced up to 10^5-fold [8]. In such a hot spot, the conventional selection rules of optical transitions are broken because of high gradient intensity of the strongly localized field [9–11]. In addition to the potential as the optical antenna, surface plasmon has a potential to combine an enormous capacity of photonics and a miniaturization of electronics [12–14]. However, due to the large radiative and nonradiative losses of the plasmon [15–17], it is difficult to efficiently excite nanomaterials by weak light. If the losses in the antenna are successfully suppressed, we can expect the antenna-assisted system to be applied to key technologies in quantum information, communication, and computation such as visible-to-telecom frequency conversion of single photons emitted by a quantum dot [18] and single-photon switch [19,20].

In the previous paper, we theoretically demonstrated optical linear responses on an antenna-molecule coupled system and reported that the molecule efficiently absorbs the incident light energy with the loss in the antenna suppressed. This is because

the interference in the coupled modes suppresses the photon absorption in the metal [21,22]. Moreover, we revealed that this phenomenon is significantly beneficial in nonlinear optical responses [23]. As a next step toward applications, we have to explore the way to enhance the total scattering probability between the antenna-molecule coupled system and photons. Because the wavelength of the photon is much larger than the size of the coupled system, the antenna effect is limited. In order to overcome the difficulty, we consider a larger antenna-molecule coupled system involving more than one molecule. However, the presence of more than one molecule seems to disturbs nonlinear processes because of the inhibition of photon-photon interaction in individual molecules, i.e., the optical nonlinearity requires incident light with higher intensity.

In this paper, we analyze the upconversion process by two photons in more than one molecule coupled to an optical antenna in order to investigate the effect of the presence of the multimolecules. In consequence, we confirm that the upconversion probability under two-photon irradiation decreases with increasing the number of molecules. However, we also find that the upconversion efficiently occurs at the optimal intermolecule coupling. This is because the intermolecule coupling lifts the degeneracy of the energy levels of the molecular system so that the inhibition of photon-photon interaction in individual molecules could be avoided. Recently, we reported that the radiation-induced coupling between molecules nearby a metallic nanostructure can become considerable even when the intermolecule distance is tens of nanometers [24]. This means that the intermolecule coupling in a large antenna-molecule system is achievable. These results indicate that controlling the intermolecule coupling provides high-efficient few-photon nonlinear responses even in the multi-molecular system without increasing the photon number. In addition, utilizing photons with quantum correlation for two-photon processes has attracted much attention in terms of not only basic science but also applications [25–30], because entangled photons are key issues in quantum information technology [31], and the generation efficiency of them is largely growing recently [32–35]. Therefore, we also examine the dependence of nonlinear optics on photon correlations and find that the correlated photons facilitate the upconversion process.

---

[*]y_osaka_opu@yahoo.co.jp
[†]yokoshi@pe.osakafu-u.ac.jp

The paper is organized as follows. In Sec. II, we introduce the theoretical formalism to analyze the two-photon upconversion process in the system where more than molecule is coupled to a metallic nanoantenna. In Sec. III, we show the numerically calculated upconversion probability, which is enhanced in the suitable conditions, and then discuss the essence of the enhancement. We also investigate the dependence of upconversion on the correlation between input photons. Our summary and conclusion are provided in Sec. IV.

II. FORMALISM

A. Multimolecular system coupled to an antenna

We consider the upconversion process by two photons in a multimolecular system coupled to an optical antenna. Although, in this section, we show the simplest case that the system contains two molecules and an optical antenna, we can also analyze the upconversion in more than two molecules in the same manner. Therefore, in the following sections, we show the results in the case that the number of molecules is two, three, and four.

In Fig. 1(a), we show one example of the system setup. The metallic nanoantenna has two hot spots near which molecules are embedded. Such a nanoantenna is actually fabricated using electron beam lithography and lift-off technique [36]. In addition, the recent progress of nanofabrication techniques enables us to prepare arrays of metallic nanostructures [37–39]. It should be noted that the typical size of the antennas is of the order of 100 nm, which is small compared to a spatial extent of photons. Therefore, even though the antenna includes more than one and separated hot spots, the excitation by a single photon must be regarded as a single surface plasmon.

Here, we consider a simplified model shown in Fig. 1(b) (in the case of two molecules). The antenna mode is modeled by simple boson with the plasmon resonance frequency ω_p and the large radiative decay rate Γ_p. The molecule A(B) is considered as a three-level system, in which the states $|m_{A(B)}\rangle$ and $|e_{A(B)}\rangle$ are dipole allowed from the ground state $|g_{A(B)}\rangle$, and the transition between the state $|e_{A(B)}\rangle$ and $|m_{A(B)}\rangle$ is dipole forbidden owing to the parity of the wave function. The radiative decay rates of the molecule A(B) are denoted by $\{\gamma_{1_{A(B)}}, \gamma_{2_{A(B)}}, \Gamma_{3_{A(B)}}\}$, where the rates of the forbidden transitions $\gamma_{2_{A(B)}}$ are much smaller than the ones of the allowed transitions $\{\gamma_{1_{A(B)}}, \Gamma_{3_{A(B)}}\}$.

The resonant energy of the plasmon depends on the size of the metal; as the metal becomes larger, the resonant energy becomes redshifted. The constant $g_{p_{A(B)}}$ denotes the coupling between the molecule A(B) and the surface plasmon at the hot spot. Because the size and the intensity of the localized electric field depends on the size and geometry of the metal, we can control the coupling by choosing the nanostructure as well as on the position of the molecules [5]. We model also the molecule-molecule coupling by the constant g_M. The origin of g_M is the free propagating photon between the molecules. The propagation direction is perpendicular to the polarization induced in the molecule. In Ref. [24], considering a similar system as in Fig. 1(a), we showed that the radiation-induced molecule-molecule coupling can be as large as $g_{p_{A(B)}}$ ($\sim$ meV) when the radiated photon is efficiently absorbed by the
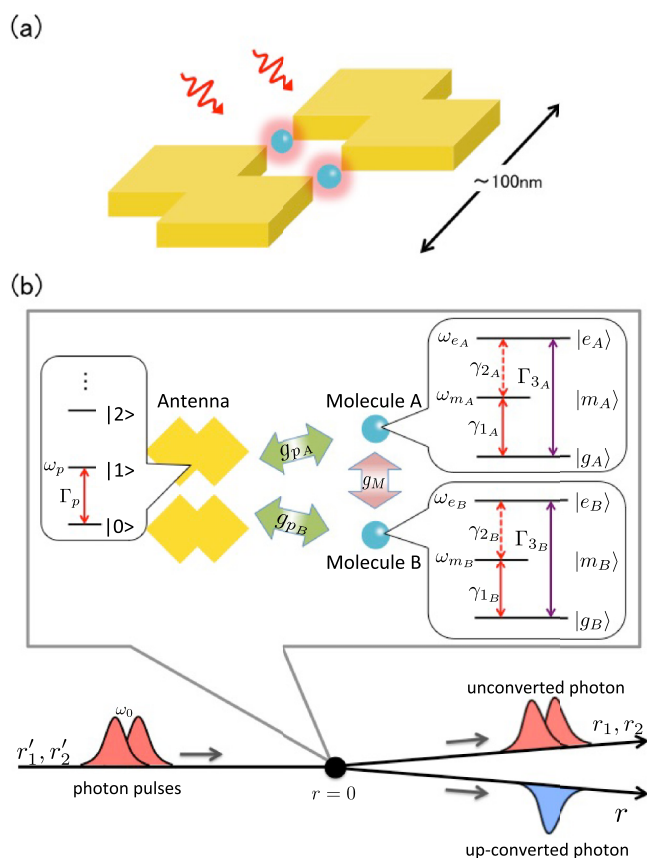

FIG. 1. (a) Illustration of one example of the optical nanoantenna structure that couples to two molecules. (b) Schematic illustration of the coupled antenna-molecules system. The localized cavity mode with large relaxation constant Γ_p excites the four-level molecule. The relaxation constants in the molecule A(B) $\{\gamma_{1_{A(B)}}, \gamma_{2_{A(B)}}, \gamma_{3_{A(B)}}\}$ are set to be much smaller compared with Γ_p. The constant g_{p_A, p_B} and g_M denote the antenna-molecule and the molecule-molecule coupling, respectively.

molecules at the hot spots. There are other various proposals to make the enhanced dipole-dipole coupling, e.g., between the molecules nearby a metal nanoparticle [40]. When the dipoles are coupled with graphene surface plasmon, by changing their relative distance, it is possible to increase or decrease the coupling between them [41]. Therefore, to some extent, we can control the system parameters by designing the metal nanostructures and the positions of molecules.

Based on the above consideration, we employ the total Hamiltonian as follows

$$\mathcal{H} = \mathcal{H}_{\text{antenna}} + \mathcal{H}_{\text{molecule}} + \mathcal{H}_{\text{photon}} \\ + \mathcal{H}_{\text{a-p}} + \mathcal{H}_{\text{m-p}} + \mathcal{H}_{\text{a-m}} + \mathcal{H}_{\text{m-m}}. \quad (1)$$

Here the energy of the antenna mode is described as $\mathcal{H}_{\text{antenna}} = \hbar\omega_p p^\dagger p$, where the operator $p^{(\dagger)}$ annihilates (creates) an antenna mode. As for the molecules, the Hamiltonian is $\mathcal{H}_{\text{molecule}} = \hbar\omega_{m_A}\sigma_{Amm} + \hbar\omega_{e_A}\sigma_{Aee} + \hbar\omega_{m_B}\sigma_{Bmm} + \hbar\omega_{e_B}\sigma_{Bee}$, in which $\sigma_{A(B)ij} = |i_{A(B)}\rangle\langle j_{A(B)}|$ with $\{i, j\} = \{g, m, e\}$ and the resonant energies are measured from the ground state $|g_{A(B)}\rangle$. We employ the one-dimensional model and then the energy of the photon field can be described as

$\mathcal{H}_{\text{photon}} = \int dk\hbar ck(\tilde{a}_k^\dagger \tilde{a}_k + \tilde{b}_k^\dagger \tilde{b}_k)$. Here the operator $b_r^{(\dagger)}$ annihilates (creates) an upconverted photon at position r and $a_r^{(\dagger)}$ annihilates (creates) an input or unconverted output photon. The tilde on the operators indicates Fourier transformation, e.g., $\tilde{a}_k = \sqrt{1/2\pi} \int dr a_r e^{-ikr}$. Input two photons interact with the coupled system at the origin ($r = 0$). The antenna-photon coupling is written within rotating-wave approximation as

$$\mathcal{H}_{\text{a-p}} = i\hbar\sqrt{c\Gamma_p}(p^\dagger a_{r=0} - a_{r=0}^\dagger p). \tag{2}$$

In a similar manner, the radiations of the photons from the molecule are

$$\begin{aligned}
\mathcal{H}_{\text{m-p}} = {}& i\hbar\sqrt{c\gamma_{1_A}}\sigma_{Amg}a_{r=0} + i\hbar\sqrt{c\gamma_{2_A}}\sigma_{Aem}a_{r=0} \\
& + i\hbar\sqrt{c\gamma_{1_B}}\sigma_{Bmg}a_{r=0} + i\hbar\sqrt{c\gamma_{2_B}}\sigma_{Bem}a_{r=0} \\
& + i\hbar\sqrt{c\Gamma_{3_A}}\sigma_{Aeg}b_{r=0} + i\hbar\sqrt{c\Gamma_{3_B}}\sigma_{Beg}b_{r=0} + \text{H.c.}
\end{aligned} \tag{3}$$

The interaction of the molecules with the plasmon field is described as

$$\begin{aligned}
\mathcal{H}_{\text{a-m}} = {}& \hbar g_{p_A}(\sigma_{Amg}p + \sigma_{Aem}p) \\
& + \hbar g_{p_B}(\sigma_{Bmg}p + \sigma_{Bem}p) + \text{H.c.}
\end{aligned} \tag{4}$$

Here we assume that the plasmon couples with both the dipole-allowed and -forbidden states because the localized electric field has steep spatial gradient [9–11]. One may think that such a situation is difficult to realize in real experiment. However, by designing the system setup properly, it is possible to excite both the states with the same extent [23]. The molecule-molecule interaction via the radiation field is written as

$$\begin{aligned}
\mathcal{H}_{\text{m-m}} = {}& \hbar g_M(\sigma_{Amg}\sigma_{Bgm} + \sigma_{Amg}\sigma_{Bme} \\
& + \sigma_{Aem}\sigma_{Bgm} + \sigma_{Aem}\sigma_{Bme}) + \text{H.c.}
\end{aligned} \tag{5}$$

We have considered the system as in Fig. 1(a). Thus, as was shown in Ref. [24] we can set the molecule-molecule coupling as large as the plasmon-molecule coupling even when the molecules are separated by tens of nanometers. We analyze the upconversion process by applying the input-output formalism to this model.

B. Upconversion process

As an initial state, we consider a two-photon state. Then, the initial state vector is written as

$$|\Psi_{\text{in}}\rangle = \iint dr_1' dr_2' \frac{f(r_1', r_2')}{\sqrt{2!}} a_{r_1'}^\dagger a_{r_2'}^\dagger |V\rangle. \tag{6}$$

On the other hand, the output state is a superposition of an upconverted photon state and two-photon state. Therefore, the output state vector can be written as

$$\begin{aligned}
|\Psi_{\text{out}}\rangle &= e^{-i\mathcal{H}t}|\Psi_{\text{in}}\rangle \\
&= \int_0^\infty dr\, h(r;\tau) b_r^\dagger |V\rangle \\
&\quad + \iint_0^\infty dr_1 dr_2 \frac{g(r_1, r_2; \tau)}{\sqrt{2!}} a_{r_1}^\dagger a_{r_2}^\dagger |V\rangle.
\end{aligned} \tag{7}$$

Here the wave function of the upconverted photon can be written as

$$\begin{aligned}
h(r;\tau) &= \langle V|b_r|\Psi_{\text{out}}\rangle = \langle V|b_r(\tau)|\Psi_{\text{in}}\rangle \\
&= \iint dr_1' dr_2' G_{\text{uc}}(r, r_1', r_2'; \tau) f(r_1', r_2'),
\end{aligned} \tag{8}$$

where $b_r(\tau) = e^{i\mathcal{H}\tau} b_r e^{-i\mathcal{H}\tau}$ (Heisenberg picture), and $G_{\text{uc}}(r, r_1', r_2'; \tau)$ is the propagator for the upconversion process, which is defined by

$$G_{\text{uc}}(r, r_1', r_2'; \tau) = \frac{\langle V|b_r(\tau) a_{r_1'}^\dagger a_{r_2'}^\dagger |V\rangle}{\sqrt{2}}. \tag{9}$$

We derive the propagator in order to gain the wave function of the upconverted photon. In the same manner, the propagator for the two-photon emission process is given as

$$G_{\text{two}}(r_1, r_2, r_1', r_2'; \tau) = \frac{\langle V|a_{r_1}(\tau) a_{r_2}(\tau) a_{r_1'}^\dagger a_{r_2'}^\dagger |V\rangle}{2}. \tag{10}$$

In calculating the propagators, we employ the method developed in Ref. [42], in which a coherent state of the photon field is introduced. According to this method, we define the coherent state as

$$|\phi\rangle = \mathcal{N} \exp(\mu_1 a_{r_1'}^\dagger + \mu_2 a_{r_2'}^\dagger)|V\rangle, \tag{11}$$

where $\mathcal{N}$ is normalization factor and $\mu_{1,2}$ are perturbation coefficients. For the above state, one can write down the relations

$$a_r|\phi\rangle = \sum_{j=1,2} \mu_j \delta(r - r_j')|\phi\rangle, \tag{12}$$

$$b_r|\phi\rangle = 0. \tag{13}$$

From the Heisenberg equations for the operators of the photons, output fields are obtained as

$$\begin{aligned}
a_r(\tau) = {}& a_{r-c\tau}(0) - \left\{ \sqrt{\frac{\Gamma_p}{c}} p\left(\tau - \frac{r}{c}\right) + \sqrt{\frac{\gamma_{1_A}}{c}} \sigma_{Agm}\left(\tau - \frac{r}{c}\right) \right. \\
& + \sqrt{\frac{\gamma_{2_A}}{c}} \sigma_{Ame}\left(\tau - \frac{r}{c}\right) + \sqrt{\frac{\gamma_{1_B}}{c}} \sigma_{Bgm}\left(\tau - \frac{r}{c}\right) \\
& \left. + \sqrt{\frac{\gamma_{2_B}}{c}} \sigma_{Bme}\left(\tau - \frac{r}{c}\right) \right\} \left\{ \theta\left(\frac{r}{c}\right) - \theta\left(\frac{r}{c} - \tau\right) \right\},
\end{aligned} \tag{14}$$

$$\begin{aligned}
b_r(\tau) = {}& b_{r-c\tau}(0) \\
& - \left(\sqrt{\frac{\Gamma_{3_A}}{c}} \sigma_{Age}\left(\tau - \frac{r}{c}\right) + \sqrt{\frac{\Gamma_{3_B}}{c}} \sigma_{Bge}\left(\tau - \frac{r}{c}\right) \right) \\
& \times \left\{ \theta\left(\frac{r}{c}\right) - \theta\left(\frac{r}{c} - \tau\right) \right\},
\end{aligned} \tag{15}$$

where $\theta(\tau)$ is the Heaviside step function. From Eqs. (9) and (15), we find the propagator for the upconversion process

to be

$$
\begin{aligned}
&G_{uc}(r_1',r_2',r;\tau)\\
&= \frac{\langle b_r(\tau)\rangle^{\mu_1\mu_2}}{\sqrt{2}}\\
&= -\sqrt{\frac{\Gamma_{3_A}}{2c}}\langle \sigma_{Age}\left(t-\frac{r}{c}\right)\rangle^{\mu_1\mu_2}\left\{\theta\left(\frac{r}{c}\right)-\theta\left(\frac{r}{c}-t\right)\right\}\\
&\quad -\sqrt{\frac{\Gamma_{3_B}}{2c}}\langle \sigma_{Bge}\left(t-\frac{r}{c}\right)\rangle^{\mu_1\mu_2}\left\{\theta\left(\frac{r}{c}\right)-\theta\left(\frac{r}{c}-t\right)\right\},
\end{aligned}
$$
(16)

where $\langle b_r(\tau)\rangle^{\mu_1\mu_2}$ means the perturbation component of proportional to $\mu_1\mu_2$ in $\langle b_r(\tau)\rangle = \langle \phi|b_r(\tau)|\phi\rangle$. Therefore, we can calculate the wave function of the upconverted photon when we get $\langle \sigma_{Age}(\tau)\rangle^{\mu_1\mu_2}$ and $\langle \sigma_{Bge}(\tau)\rangle^{\mu_1\mu_2}$.

We can obtain time evolution equations for the operators from Heisenberg equations, for example,

$$
\frac{d}{d\tau}\sigma_{Age}(\tau) = \frac{i}{\hbar}[\mathcal{H},\sigma_{Age}(\tau)].
$$
(17)

From the above equation, the equation for the expectation value of the operator $\sigma_{Age}(\tau)$, i.e., $\langle \sigma_{Age}(\tau)\rangle$ is obtained. Furthermore, the equation of motion for $\langle \sigma_{Age}(\tau)\rangle^{\mu_1\mu_2}$ can be written as

$$
\begin{aligned}
&\frac{d}{dt}\langle \sigma_{Age}(\tau)\rangle^{\mu_1\mu_2}\\
&= -\left(i\omega_{e_A}+\frac{\Gamma_{3_A}+\gamma_{2_A}}{2}\right)\langle \sigma_{Age}(\tau)\rangle^{\mu_1\mu_2}\\
&\quad -\left(ig_{p_A}+\frac{\sqrt{\gamma_{2_A}\Gamma_p}}{2}\right)\langle \sigma_{Agm}(\tau)p(\tau)\rangle^{\mu_1\mu_2}\\
&\quad +\sqrt{c\gamma_{2_A}}\langle \sigma_{Agm}(\tau)\rangle^{\mu_2}\delta(c\tau+r_1')\\
&\quad +\sqrt{c\gamma_{2_A}}\langle \sigma_{Agm}(\tau)\rangle^{\mu_1}\delta(c\tau+r_2')\\
&\quad -\left(ig_{M_{21}}+\frac{\sqrt{\gamma_{2_A}\gamma_{1_B}}}{2}\right)\langle \sigma_{Agm}(\tau)\sigma_{Bgm}(\tau)\rangle^{\mu_1\mu_2}\\
&\quad -\frac{\sqrt{\Gamma_{3_A}\Gamma_{3_B}}}{2}\langle \sigma_{Bge}(\tau)\rangle^{\mu_1\mu_2},
\end{aligned}
$$
(18)

where we have used the relations of Eqs. (14) and (15) and ignored the components having no contribution to $\langle \sigma_{Age}(\tau)\rangle^{\mu_1\mu_2}$. In the same manner, we can write down the equations of motion for other operators. Using initial conditions, e.g., $\langle \sigma_{Age}(0)\rangle^{\mu_1\mu_2} = 0$, we have solved these simultaneous equations and then determined the propagator by substituting the solutions into Eq. (16). Then, the upconversion probability P_{uc} and two-photon emission probability P_{two} are calculated as

$$
P_{uc} = \int dr |h(r;\tau)|^2,
$$
(19)

$$
P_{two} = \iint dr_1 dr_2 |g(r_1,r_2;\tau)|^2,
$$
(20)

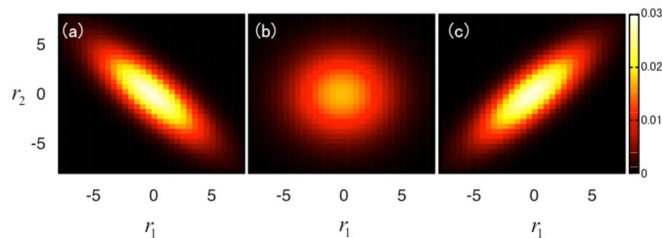where they satisfy $P_{uc} + P_{two} = 1$.

FIG. 2. Density plots of the input two-photon wave function of (a) spatially anticorrelated ($\rho = -0.8$), (b) spatially uncorrelated ($\rho = 0$), and (c) spatially correlated ($\rho = 0.8$) states.

C. Input two-photon with correlation

It is known that correlated photons enhance two-photon process owing to allowing simultaneous excitations, thus utilizing of photons with quantum correlation for two-photon processes has attracted much attention [25–30]. Besides, because entangled photons are key issues in quantum information technology [31], the study of nonlinear responses by the correlated photons is not only interesting in itself, but also can contribute to further development in photoscience. Therefore, in order to discuss the effect of the photon correlation for the nonlinear process, we assume that the input two-photon wave function is expressed by bi-variable Gaussian pulse as

$$
f(r_1,r_2) = \frac{\exp\left[-\frac{\bar{r}_1^2+\bar{r}_2^2-2\rho\bar{r}_1\bar{r}_2}{4(1-\rho^2)d^2} + i\frac{\omega_0}{c}(\bar{r}_1+\bar{r}_2)\right]}{(2\pi)^{1/2}d(1-\rho^2)^{1/4}}, \quad (21)
$$

where $\bar{r} = r - a$ is the distance from the initial position a, and the parameter ρ denotes the correlation between two photons. The pulse length d corresponds to the temporal coherence length of the photon, and recent experiments reported that entangled photons or single photon sources generate photons with the long coherence length of $10^{-4}\sim10^2$ m [43–48]. Although the coherence length of sunlight is approximately several hundreds of nanometers [49], photons with that of the order of cm are obtained by the spectral filtering technique [50]. The frequency of the pulse ω_0 is set to the localized surface plasmon resonance. Figure 2 shows the density plots $|f(r_1,r_2)|^2$ for the wave function at (a) $\rho = -0.8$, (b) $\rho = 0$, and (c) $\rho = 0.8$. When the correlation parameter ρ is equal to 0, the input two photons can be decoupled. On the other hand, as ρ gets close to 1 (-1), they are in a strongly correlated (anticorrelated) state. Such an entangled photon-pair can be actually generated using spontaneous parametric down-conversion [35]. We discuss the dependence of upconversion processes on the correlation of input two-photon in Sec. III C. In other sections, we assume that input two-photon is noncorrelated, i.e., $\rho = 0$.

III. ENHANCED UPCONVERSION

We numerically calculate the probability of the upconversion in molecules coupled to an antenna. Hereafter we basically assume that the frequencies of the plasmon mode and molecules are set to be $\omega_p = \omega_{m_A,m_B} = \omega_{e_A,e_B}/2$. Because the relaxation constant of the plasmon mode is large compared to the other rates, we use $\Gamma_{3_A,3_B}/\Gamma_p = 0.2$, $\gamma_{1_A,1_B}/\Gamma_p = 0.01$, $\gamma_{2_A,2_B}/\Gamma_p = 0.001$. In addition, for simplicity, we assume that
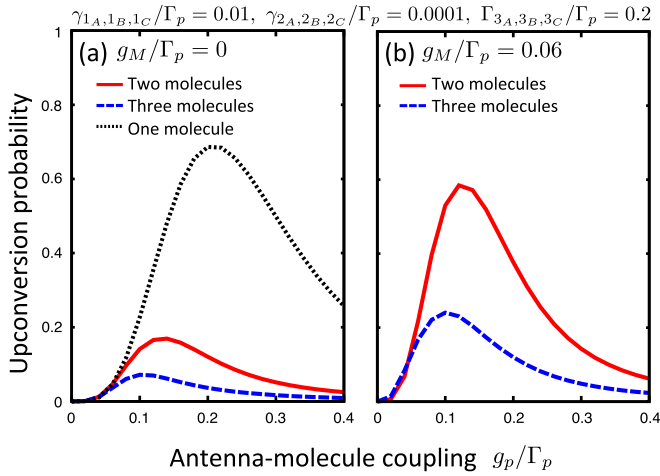
FIG. 3. Probability of upconversion is plotted against the antenna-molecule coupling at the intermolecule coupling constant (a) $g_M = 0$ and (b) $g_M/\Gamma_p = 0.06$. The solid, dashed, and dotted lines express the probability in the case that the quantum complex system contains two molecules, three molecules, and one molecule, respectively. We find that although the probability reduces with increasing the number of the molecules, the intermolecule coupling enhances the probability.

both the antenna-molecule coupling constants are equal, i.e., $g_{P_A} = g_{P_B} = g_p$. We set the pulse length to be $d\Gamma_p/c = 7$, which corresponds to $d = 434\ \mu$m for $\hbar\Gamma_p = 20$ meV.

A. Effect of intermolecule correlation

We investigate the effects of the presence of more than one molecule on the upconversion process. The probability of the upconversion for intermolecule coupling $g_M = 0$ is shown in Fig. 3(a). In the case of containing one molecule within the quantum complex system (black dotted line), we can see that the probability is enhanced at the optimal antenna-molecule coupling, where the loss of the antenna is suppressed by the quantum interference [23]. However, as the number of the molecules within the quantum system increases, the upconversion probability decreases. This is because the second and third molecules inhibit the process of two photons in a molecule. On the other hand, Figure 3(b) shows the probability of the upconversion for intermolecule coupling $g_M/\Gamma_p = 0.06$. In comparison with Fig. 3(a), it is found that the intermolecule coupling enhances the probability. In order to examine the coupling dependence of the upconversion process, we show the probability as a function of the molecule-molecule coupling. At first, we consider the upconversion in two molecules, which are coupled to an antenna. Figure 4 shows the probability plotted against the antenna-molecule and molecule-molecule coupling and reveals that the upconversion is enhanced at both the optimal couplings. In Fig. 5, the probability is calculated as functions of the molecule-molecule coupling g_M and the detuning of the input photon energy from the resonances of the plasmon and the molecule. This result states that the optimal range of the coupling depends on the frequency detuning. Figure 6 shows the couplings dependence of the upconversion probability in the case of containing more than two molecules within the coupled system. As is the case
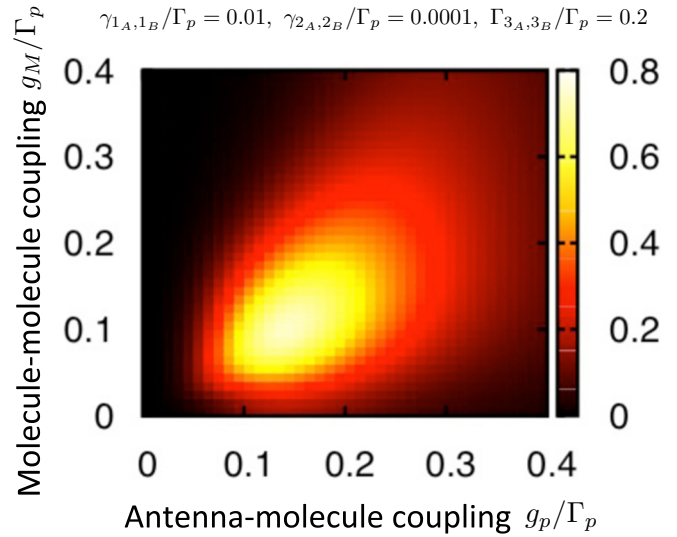

FIG. 4. Coupling dependence of the upconversion probability on the two molecules, which are coupled to an antenna. The probability is plotted against the antenna-molecule coupling g_p and the molecule-molecule coupling g_M. We find the optimal ranges for both the couplings.

in Fig. 4, it is confirmed that there are the optimal ranges of both couplings. These results mean that controlling both the antenna-molecule and the intermolecule couplings leads to high-efficient upconversion even though the number of molecule is more than two.

B. Essence of enhancement

We discuss the essence of the enhancement at the optimal intermolecule coupling. Here, for simplified discussions, we
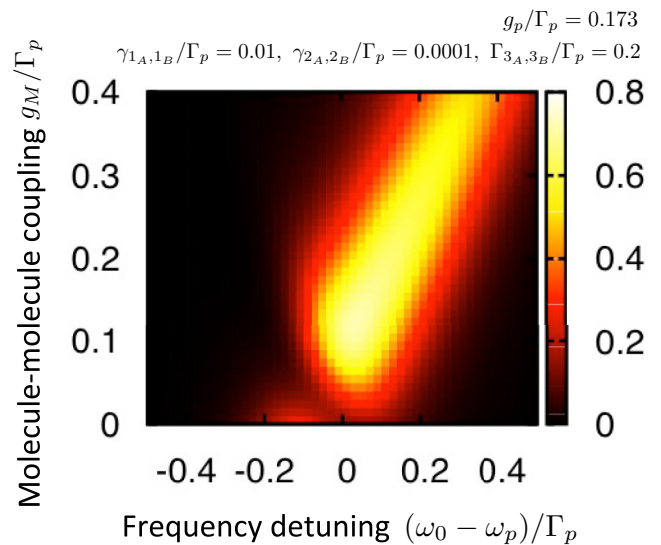

FIG. 5. Frequency detuning dependence of the upconversion probability on the two molecules coupled to an antenna. The probability is shown as functions of the molecule-molecule coupling g_M and the frequency detuning of the input photon from the resonances of the plasmon and the molecule. It is found that the optimal range of the coupling depends on the frequency detuning.
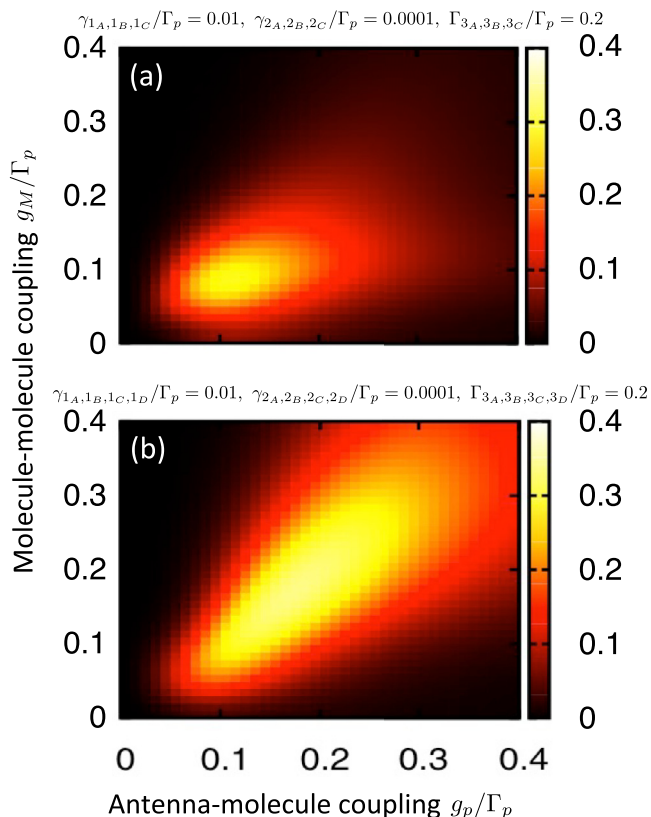
FIG. 6. Upconversion probability is plotted against the antenna-molecule coupling g_p and the molecule-molecule coupling g_M in the case of containing (a) three molecules and (b) four molecules within the coupled system.
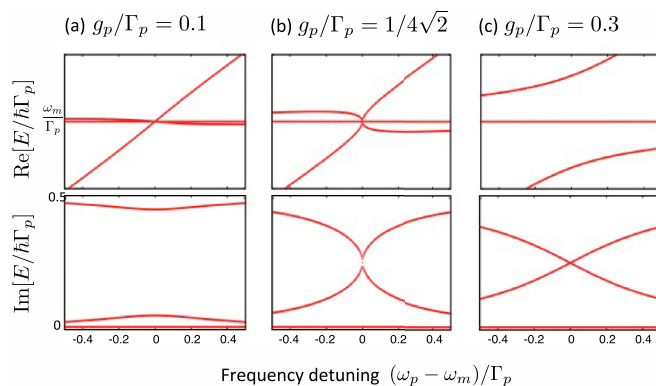

FIG. 7. Eigenvalues of the coupled modes for the antenna-molecule coupling constant (a) $g_p/\Gamma_p = 0.1$, (b) $g_p/\Gamma_p = 1/4\sqrt{2}$, and (c) $g_p/\Gamma_p = 0.3$. Here the intermolecule coupling is fixed to $g_M = 0$. The horizontal axis is the detuning between the resonant frequency of the antenna mode and that of the first excited state of the molecule $|m_{A(B)}\rangle$. The upper (lower) three figures show the real (imaginary) part of the eigenmodes. This complex frequency of the dark mode is always constant because it does not include the antenna mode. In the upper figures, one can find an anticrossing (Rabi splitting) when g_p/Γ_p is larger than $1/4\sqrt{2}$. On the other hand, when g_p/Γ_p is smaller than $1/4\sqrt{2}$, one can find a crossing. Then, the energies of upper and lower branches become equal at $\omega_p = \omega_m$. In the lower figures, one can find a crossing when g_p/Γ_p is larger than $1/4\sqrt{2}$. Then, the radiative decay rates of upper and lower branches become equal at $\omega_p = \omega_m$. Therefore, the two bright modes oscillate in the same frequency and with the same time constant at $g_p/\Gamma_p = 1/4\sqrt{2}$ and $\omega_p = \omega_m$. This is the condition for the quantum interference in the coupled system.

ignore the radiative decay rates of the molecules, i.e., $\gamma_{1_A,1_B} = \gamma_{2_A,2_B} = \Gamma_{3_A,3_B} = 0$. In addition, the resonance energies of the two molecules are equal to each other, i.e., $\omega_{m_A} = \omega_{m_B} = \omega_m$, $\omega_{e_A} = \omega_{e_B} = \omega_e$.

The eigenmodes of the coupled system for the different antenna-molecule coupling constants g_p is shown in Fig. 7, where the intermolecule coupling is fixed to $g_M = 0$. The upper (lower) three figures show the real (imaginary) part of eigenmodes, which corresponds to the frequency (decay rate) of the coupled modes. Here, this complex frequency of the dark mode is always constant because it does not include the antenna mode. The other two modes efficiently interfere constructively and destructively at the crossing point, which appears at the optimal antenna-molecule coupling. This is because the two modes oscillate in the same frequency and with the same time constant. Owing to this quantum interference in the coupled system, when the destructive interference occurs in the antenna mode, it is possible to make only the molecular polarization oscillate. Then, the large loss in antenna is suppressed and we can achieve the efficient few-photon nonlinear responses [23]. However, in the case that more than one molecule is present, these conditions are not sufficient to induce the high-efficient upconversion. The reason is explained as follows. Because two photons interact with a number of molecules, the expected values of the population of the individual molecules decrease. Therefore, whereas

photons efficiently excite a number of molecules owing to this quantum interference, strong photon-photon interaction in one molecule, which is of importance to nonlinear optical processes, is inhibited. Figure 3(a) corresponds to the above case.

Figure 8 shows the real and imaginary parts of the eigenmodes for the different molecule-molecule coupling constants g_M, where antenna-molecule coupling is fixed to $g_p = 1/4\sqrt{2}$. From the upper and lower figures, one can see that the crossing point shifts with increasing the molecule-molecule coupling. This shift is due to the splitting of the molecular modes induced by the intermolecule coupling. Actually, Figure 5 shows that the optimal energy of input photons for the upconversion moves to the higher frequency side with increasing the intermolecule coupling. From these results, we interpret that the degeneracy of the molecular levels is lifted by the intermolecule coupling. Then, it is possible to excite only one of the eigenmodes, which avoids the inhibition of the photon-photon interaction in the molecules. Therefore, by controlling both the antenna-molecule coupling and the molecule-molecule coupling, we can achieve the efficient few-photon nonlinear responses in the presence of a number of the molecule.

C. Dependence on correlation of input photons

We discuss the dependence of the upconversion on correlations between input two photons. In Fig. 9(a), the upconversion
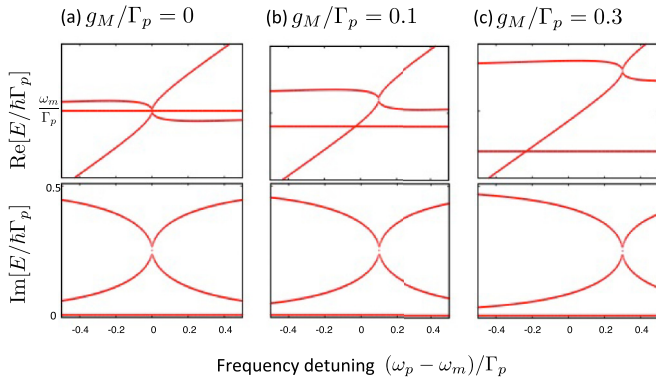
FIG. 8. Eigenvalues of the coupled modes for the antenna-molecule coupling constant (a) $g_M/\Gamma_p = 0$, (b) $g_M/\Gamma_p = 0.1$, and (c) $g_M/\Gamma_p = 0.3$. Here the antenna-molecule coupling is fixed to $g_p = 1/4\sqrt{2}$. The horizontal axis is the detuning between the resonant frequency of the antenna and that of the first excited state of the molecule $|m_{A(B)}\rangle$. The upper (lower) three figures show the real (imaginary) part of the eigenmodes. In the upper figures, it is found that the crossing point shifts due to the splitting of the mode frequencies induced by the molecule-molecule coupling. Accordingly, we can access only one of the eigenmodes resonantly.

probability is plotted as a function of the input two-photon correlation and the antenna-molecule coupling. In Fig. 9(b), the probability is plotted as a function of the input two-photon correlation and the molecule-molecule coupling. These figures show that the upconversion process is facilitated when input two photons are correlated in space, i.e., the correlation parameter ρ is close to 1. This is because the spatial correlation allows two photons to interact the coupled system almost simultaneously and excite the molecules sequentially. The sequential excitation is of importance to the upconversion process. Accordingly, the correlation of input photons spreads the optimal regime of the antenna-molecule and molecule-molecule coupling for the efficient upconversion.

IV. CONCLUSION

A larger antenna-molecule coupled system, which involves more than one molecule, is suitable in order to enlarge the total scattering probability between photons with micrometer-scale wavelength and molecules nearby nanometer-scale metallic antennas. However, the presence of multiple molecules seems to damage nonlinear optical processes because of the inhibition of photon-photon interaction in one molecule, when the system is irradiated by weak light, which contains only a few photons. Therefore, we have theoretically studied two-photon upconversion in a quantum complex system where more than one molecule is coupled to a metallic nanoantenna. As a result, we have confirmed that the probability decreases with increasing the number of the molecules. However, we have
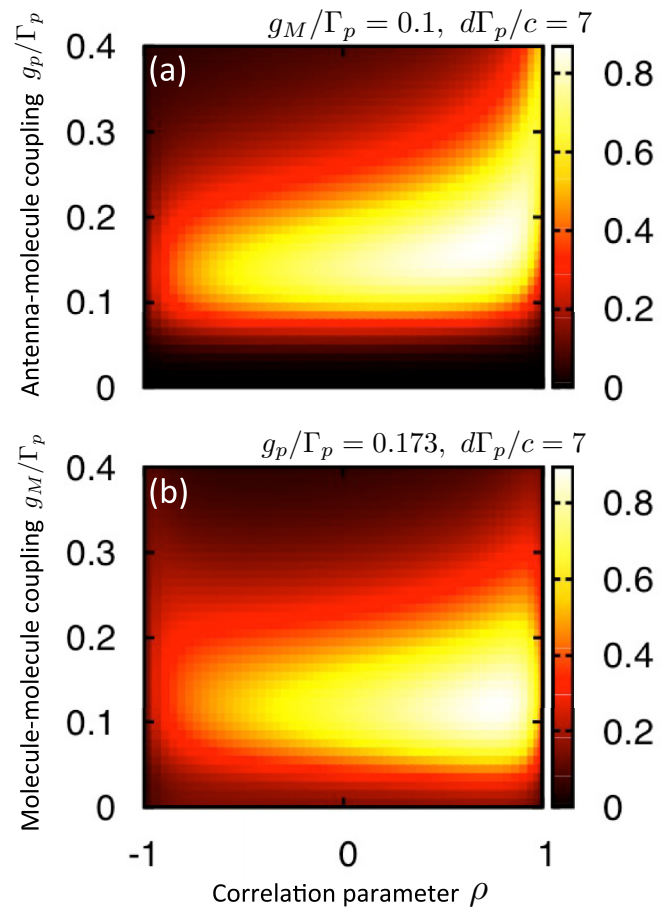

FIG. 9. Dependence of the upconversion on the input photon-correlation. (a) The upconversion probability is plotted as a function of input photon correlation and antenna-molecule coupling at $g_M/\Gamma_p = 0.1$. (b) The probability is plotted as a function of input photon correlation and molecule-molecule coupling at $g_p/\Gamma_p = 0.173$. When input two photons are correlated in space (i.e., ρ is close to 1), the upconversion process is facilitated.

shown that controlling the intermolecule coupling, which is enhanced near the metallic nanoantenna, resolves the difficulty by lifting the degeneracy of the energy levels of the molecular system. Therefore the total design of the antenna-molecule and intermolecular coupling enhances few-photon nonlinear responses in the large antenna-molecule coupled system. These results will open avenues for nonlinear optical devices to realize single-photon control techniques, e.g., wavelength conversion of single photons and single photon switching.

[1] D. S. Chemla and D. A. B. Miller, Opt. Lett. **11**, 522 (1986).

[2] K. J. Vahala, Nature (London) **424**, 839 (2003).

[3] B. Deveaud, *The Physics of Semiconductor Microcavities* (Wiley-VCH, Weinheim, 2007).

[4] P. Muehlschlegel, H.-J. Eisler, O. J. F. Martin, B. Hecht, and D. W. Pohl, Science **308**, 1607 (2005).

[5] P. Bharadwaj, B. Deutsch, and L. Novotny, Adv. Opt. Photon. **1**, 438 (2009).

[6] P. Anger, P. Bharadwaj, and L. Novotny, Phys. Rev. Lett. **96**, 113002 (2006).

[7] A. Kinkhabwala, Z. Yu, S. Fan, Y. Avlasevich, K. Müllen, and W. E. Moerner, Nat. Photon. **3**, 654 (2009).

[8] E. Hao and G. C. Schatz, J. Chem. Phys. **120**, 357 (2004).

[9] T. Iida and H. Ishihara, Phys. Status Solidi A **206**, 980 (2009).

[10] P. K. Jain, D. Ghosh, R. Baer, E. Rabani, and A. P. Alivisatos, Proc. Natl. Acad. Sci. USA **109**, 8016 (2012).

[11] M. Takase, H. Ajiki, Y. Mizumoto, K. Komeda, M. Nara, H. Nabika, S. Yasuda, H. Ishihara, and K. Murakoshi, Nat. Photon. **7**, 550 (2013).

[12] W. L. Barnes, A. Dereux, and T. W. Ebbesen, Nature (London) **424**, 824 (2003).

[13] E. Ozbay, Science **311**, 189 (2006).

[14] H. A. Atwater, Sci. Am. **296**, 56 (2007).

[15] M. I. Stockman, Opt. Express **19**, 22029 (2011).

[16] F. Stietz, J. Bosbach, T. Wenzel, T. Vartanyan, A. Goldmann, and F. Träger, Phys. Rev. Lett. **84**, 5644 (2000).

[17] C. Sönnichsen, T. Franzl, T. Wilk, G. von Plessen, J. Feldmann, O. Wilson, and P. Mulvaney, Phys. Rev. Lett. **88**, 077402 (2002).

[18] S. Zaske, A. Lenhard, C. A. Keßler, J. Kettler, C. Hepp, C. Arend, R. Albrecht, W.-M. Schulz, M. Jetter, P. Michler, and C. Becher, Phys. Rev. Lett. **109**, 147404 (2012).

[19] A. Kubanek, A. Ourjoumtsev, I. Schuster, M. Koch, P. W. H. Pinkse, K. Murr, and G. Rempe, Phys. Rev. Lett. **101**, 203602 (2008).

[20] T. Volz, A. Reinhard, M. Winger, A. Badolato, K. J. Hennessy, E. L. Hu, and A. Imamoglu, Nat. Photon. **6**, 605 (2012).

[21] H. Ishihara, A. Nobuhiro, M. Nakatani, and Y. Mizumoto, J. Photochem. Photobiol., A **221**, 148 (2011).

[22] M. Nakatani, A. Nobuhiro, N. Yokoshi, and H. Ishihara, Phys. Chem. Chem. Phys. **15**, 8144 (2013).

[23] Y. Osaka, N. Yokoshi, M. Nakatani, and H. Ishihara, Phys. Rev. Lett. **112**, 133601 (2014).

[24] Y. Osaka, N. Yokoshi, and H. Ishihara, Int. J. Antenn. Propag. **2015**, 747580 (2015).

[25] C. W. Gardiner, Phys. Rev. Lett. **56**, 1917 (1986).

[26] E. S. Polzik, J. Carri, and H. J. Kimble, Phys. Rev. Lett. **68**, 3020 (1992).

[27] N. P. Georgiades, E. S. Polzik, K. Edamatsu, H. J. Kimble, and A. S. Parkins, Phys. Rev. Lett. **75**, 3426 (1995).

[28] D.-I. Lee and T. Goodson III, J. Phys. Chem. B **110**, 25582 (2006).

[29] K. A. O'Donnell and A. B. U'Ren, Phys. Rev. Lett. **103**, 123602 (2009).

[30] H. Oka, Opt. Express **18**, 25839 (2010).

[31] M. A. Nielsen and I. L. Chuang, *Quantum Computation and Quantum Information*, 10th ed. (Cambridge University Press, New York, NY, 2011).

[32] P. G. Kwiat, K. Mattle, H. Weinfurter, A. Zeilinger, A. V. Sergienko, and Y. Shih, Phys. Rev. Lett. **75**, 4337 (1995).

[33] K. Edamatsu, G. Oohata, R. Shimizu, and T. Itoh, Nature (London) **431**, 167 (2004).

[34] C. L. Salter, R. M. Stevenson, I. Farrer, C. A. Nicoll, D. A. Ritchie, and A. J. Shields, Nature (London) **465**, 594 (2010).

[35] R. Shimizu, K. Edamatsu, and T. Itoh, Phys. Rev. A **67**, 041805 (2003).

[36] Y. Y. Tanaka, M. Komatsu, H. Fujiwara, and K. Sasaki, Nano Lett. **15**, 7086 (2015).

[37] K. Ueno, S. Juodkazis, T. Shibuya, Y. Yokota, V. Mizeikis, K. Sasaki, and H. Misawa, J. Am. Chem. Soc. **130**, 6928 (2008).

[38] V. G. Kravets, F. Schedin, and A. N. Grigorenko, Phys. Rev. Lett. **101**, 087403 (2008).

[39] B. J. Roxworthy, A. M. Bhuiya, X. Yu, E. K. C. Chow, and K. C. Toussaint Jr., Nat. Commun. **5**, 4427 (2014).

[40] V. N. Pustovit and T. V. Shahbazyan, Phys. Rev. Lett. **102**, 077401 (2009).

[41] P. A. Huidobro, A. Y. Nikitin, C. González-Ballestero, L. Martín-Moreno, and F. J. García-Vidal, Phys. Rev. B **85**, 155438 (2012).

[42] K. Koshino and M. Nakatani, Phys. Rev. A **79**, 055803 (2009).

[43] J.-W. Pan, M. Daniell, S. Gasparoni, G. Weihs, and A. Zeilinger, Phys. Rev. Lett. **86**, 4435 (2001).

[44] C. Santori, D. Fattal, J. Vuckovic, G. S. Solomon, and Y. Yamamoto, Nature (London) **419**, 594 (2002).

[45] C. Santori, D. Fattal, J. Vuckovic, G. S. Solomon, and Y. Yamamoto, New J. Phys. **6**, 89 (2004).

[46] C. E. Kuklewicz, F. N. C. Wong, and J. H. Shapiro, Phys. Rev. Lett. **97**, 223601 (2006).

[47] S. Du, P. Kolchin, C. Belthangady, G. Y. Yin, and S. E. Harris, Phys. Rev. Lett. **100**, 183603 (2008).

[48] X.-H. Bao, Y. Qian, J. Yang, H. Zhang, Z.-B. Chen, T. Yang, and J.-W. Pan, Phys. Rev. Lett. **101**, 190501 (2008).

[49] A. Donges, Eur. J. Phys. **19**, 245 (1998).

[50] P. K. Tan, G. H. Yeo, H. S. Poh, A. H. Chan, and C. Kurtsiefer, Astrophys. J. Lett. **789**, L10 (2014).